

Constraining Type Ia supernovae through their heights in edge-on galaxies

Lilit V. Barkhudaryan*

Center for Cosmology and Astrophysics, Alikhanian National Science Laboratory, 2 Alikhanian Brothers Str., 0036 Yerevan, Armenia

Accepted 2022 December 13. Received 2022 November 22; in original form 2022 September 2

ABSTRACT

In this Letter, using classified 197 supernovae (SNe) Ia, we perform an analyses of their height distributions from the disc in edge-on spirals and investigate their light-curve (LC) decline rates (Δm_{15}). We demonstrate, for the first time, that 91T- and 91bg-like subclasses of SNe Ia are distributed differently toward the plane of their host disc. The average height from the disc and its comparison with scales of thin/thick disc components gives a possibility to roughly estimate the SNe Ia progenitor ages: 91T-like events, being at the smallest heights, originate from relatively younger progenitors with ages of about several 100 Myr, 91bg-like SNe, having the highest distribution, arise from progenitors with significantly older ages ~ 10 Gyr, and normal SNe Ia, which distributed between those of the two others, are from progenitors of about one up to ~ 10 Gyr. We find a correlation between LC decline rates and SN Ia heights, which is explained by the vertical age gradient of stellar population in discs and a sub-Chandrasekhar mass white dwarf explosion models, where the Δm_{15} parameter is a progenitor age indicator.

Key words: supernovae: individual: Type Ia – galaxies: disc – galaxies: stellar content – galaxies: structure.

1 INTRODUCTION

Type Ia supernovae (SNe Ia) are known to arise from carbon–oxygen (CO) white dwarfs (WDs) in interacting close binaries. About one-third of SNe Ia contain unusual properties and divided into following main subclasses: 91T-like SNe are ~ 0.6 mag overluminous than normal SNe Ia at the B -band maximum; 91bg-like events are ~ 2 mag subluminous than normal ones (e.g. Taubenberger 2017). SNe Ia luminosities at B -band maximum and their light curve (LC) decline rates (Δm_{15} - difference between magnitudes at the maximum light and those of 15 days) are correlated (Phillips 1993): more luminous SNe Ia have slower declining LCs.

Many studies demonstrated that the progenitor population age of SN Ia subclasses is increasing in the sequence of 91T-, normal, and 91bg-like events (e.g. Howell 2001; Ashall et al. 2016). Theoretically, the progenitor age distribution at the current epoch should have a bimodal shape, with the first peak being below or close to 1 Gyr and corresponding to the young/prompt SNe Ia, and the second peak being at about several Gyr and including old/delayed events (e.g. Childress et al. 2014).

In Hakobyan et al. (2017, hereafter H17), taking into account that the height from the disc plane is an indicator of stellar population age (e.g. Seth et al. 2005; Yoachim & Dalcanton 2006; Ciucă et al. 2018), we showed that the majority of SNe Ia are localized in the discs of edge-on galaxies and they have about two times larger scale height than core-collapse (CC) SNe, whose progenitors' ages are up to ~ 100 Myr. Also, we showed that the scale height of SNe Ia is compatible with that of the older thick disc population of the Milky Way (MW) galaxy. Nevertheless, we did not investigate different subclasses of SNe Ia separately. In this Letter, for the first time, we

attempt to accomplish this by studying the distributions of heights of various SN Ia subclasses from the host discs.

Recently, in Hakobyan et al. (2020, hereafter H20), we verified an earlier finding on the correlation between LC decline rates of SNe Ia and the global ages of their host galaxies: SNe Ia from older and younger stellar populations, respectively, have larger and smaller Δm_{15} values. This result can be interpreted within the frameworks of the sub-Chandrasekhar mass ($M_{\text{Ch}} \approx 1.4M_{\odot}$) WD explosion models. The explosion mechanism is realized in the double detonation of a sub- M_{Ch} WD, in which accreted helium shell detonation initiates second detonation in the core of CO WD (e.g. Sim et al. 2010; Blondin et al. 2017; Shen et al. 2017). More luminous SNe Ia that have slower declining LCs (smaller Δm_{15} values) are produced by the explosion of more massive sub- M_{Ch} WD, because the luminosity of SN Ia is related to the mass of ^{56}Ni synthesized during the WD explosion (e.g. Stritzinger et al. 2006), which in turn is related to the mass of the WD (see e.g. Piro et al. 2014; Shen et al. 2018, for a variety of specific explosion models). On the other hand, more massive WD would come from more massive main-sequences stars, which have shorter lifetime than the progenitors of less massive WDs. In addition, due to the gravitational wave emission, massive WDs in the binary system would interact in a shorter timescale. Thus, it should follow that the LC decline rate Δm_{15} of SN Ia is correlated with the age of the SN progenitor system (e.g. Shen et al. 2017, 2021). Given this, in our study we simply check the potential correlation between the SN Ia heights from host discs and their LC decline rates, which may provide an indication that both parameters are appropriate stellar population age indicators.

2 SAMPLE SELECTION AND REDUCTION

In this study, to ensure a sufficient number of SNe and to appropriately measure the SN heights from their host galactic discs, we

* E-mail: l.barkhudaryan@yerphi.am

selected the spectroscopically classified SN Ia subclasses (normal, 91T- and 91bg-like) with distances ≤ 200 Mpc from the Open Supernova Catalog (Guillochon et al. 2017). In order to have high confidence on the SN subclasses, the information is additionally verified utilizing data from the Weizmann Interactive Supernova data REPOSITORY (Yaron & Gal-Yam 2012), Astronomer’s Telegram, website of the Central Bureau for Astronomical Telegrams, etc.¹

Since we are interested in SNe Ia that exploded in highly inclined spiral galaxies, we need to roughly classify the morphology and estimate the inclination of hosts. To perform this we employed the Sloan Digital Sky Survey Data Release 16 (DR16; Ahumada et al. 2020), the SkyMapper DR2 (Onken et al. 2019), and the Pan-STARRS DR2 (Chambers et al. 2016), which together cover the whole sky and provide the *gri* bands composed images for each host galaxy. Hosts with visible low inclinations ($i \lesssim 60^\circ$) and obviously elliptical, lenticular, or irregular morphology were excluded from the study. Following H20, we further morphologically classified the hosts and created the 25 mag arcsec⁻² elliptical apertures for each galaxy on the surveys’ *g*-band images enabling exact measurements of the SN hosts’ inclinations, semi-major (R_{25}) and semi-minor (Z_{25}) axes.

The next step was to use the estimated elongations (R_{25}/Z_{25}) and morphological types of galaxies to calculate inclinations, following the approach of Paturel et al. (1997). It is worth noting that the calculated inclinations for galaxies with prominent bulges are inaccurate, as the isophotes of bulges in highly inclined galaxies reduce the real galaxy disc inclinations. Such scenarios got special attention for exact inclination calculation, with only the isophotes of discs being taken into account (see H17). Finally, we limited the sample of host galaxies to those with an inclination of $80^\circ \leq i \leq 90^\circ$. As a result, we sampled 196 S0/a–Sdm galaxies with a nearly edge-on view, where a total of 197 SNe Ia were discovered (Table A1).

It is important to test the representativeness of our edge-on SN host sample compared to a sample of galaxies arbitrarily aligned along line-of-sight. Using the two-sample Kolmogorov–Smirnov (KS) and Anderson–Darling (AD) tests,² we compared the distributions of the sampled SN Ia subclasses and the morphological types of their hosts with the same distributions of nearly complete volume-limited (≤ 80 Mpc) sample of the Lick Observatory Supernova Search (LOSS; Li et al. 2011). In our and LOSS samples, the representations of SN Ia subclasses are not statistically different (the probabilities that the distributions are drawn from the same parent sample are > 0.6). The frequencies of morphologies in our and LOSS samples are also consistent between each other (probabilities are > 0.1). Therefore, any artificial loss or excess of SN subclasses and/or host’s morphologies should be not significant in our sample.

We used the methods described in our earlier study on edge-on SN hosts (H17) to determine the height (V) of a SN from the plane of its host disc (i.e. the vertical distance of a SN from the major axis of host), as well as the projected radius (U) along the plane. The *g*-band images were used for these measurements. The values of U and V are given in arcsec units. In this study, we used the R_{25} normalization (in arcsec) to bring the galaxies to relatively the same size (normalized height is V/R_{25} , normalized projected radius is U/R_{25}). For more details on the measurement techniques, the reader is referred to Hakobyan et al. (2016), H17. In the Appendix, we also applied Z_{25} normalization to the V parameter (V/Z_{25}).

Recall that the galaxies in our sample have an inclination of $80^\circ - 90^\circ$, which can introduce discrepancies in (projected) height

Table 1. Comparison of the positional distributions of the SN Ia subclasses along major U and minor V axes.

SN	N_{SN}	$\langle U /R_{25} \rangle$	versus	$\langle V /R_{25} \rangle$	$P_{\text{KS}}^{\text{MC}}$	$P_{\text{AD}}^{\text{MC}}$
Normal	144	$0.28^{+0.05}_{-0.04}$	versus	$0.07^{+0.01}_{-0.01}$	<0.001	<0.001
91T	30	$0.25^{+0.12}_{-0.07}$	versus	$0.05^{+0.03}_{-0.02}$	<0.001	<0.001
91bg	23	$0.25^{+0.15}_{-0.08}$	versus	$0.14^{+0.08}_{-0.04}$	0.022	0.145
All	197	$0.27^{+0.04}_{-0.03}$	versus	$0.07^{+0.01}_{-0.01}$	<0.001	<0.001

Notes. The P_{KS} and P_{AD} probabilities that the distributions are drawn from the same parent sample are calculated using a MC simulation with 10^5 iterations. Each subsample’s mean values with their 95 per cent confidence intervals (CIs) are presented. The P -values are bolded when differences between the distributions are statistically significant ($P \leq 0.05$).

measurements when compared to physical heights in the same galaxies with inclination of 90° . To check the impact of this effect, using a Monte Carlo (MC) simulation, we generated 1000 SN heights in $i = 90^\circ$ disc adopting a generalized vertical distribution ($f(\tilde{z}) = \text{sech}^2(\tilde{z}/\tilde{z}_0)$, where $\tilde{z} = V/R_{25}$) and its scale heights for SNe Ia in spiral galaxies ($\tilde{z}_0 = 0.083$; H17). Then, we randomly assigned an inclination within $80^\circ - 90^\circ$ to the disc for each SN and estimated the projected SN height from the major axis of the host. Eventually, the comparison of the generated and projected heights showed that the differences between them is not significant ($P_{\text{KS}} = 0.130$, $P_{\text{AD}} = 0.200$). Thus, the mentioned effect has a minor impact on the real height measurements, which accounts, on average, for about 10 per cent of the measured value (± 0.01 in absolute units, typically within the range of measurement errors).

Because we aim to investigate the possible relationships between photometric features like Δm_{15} and the heights of SNe Ia from the disc, following H20, we conducted a thorough literature search to assemble the *B*-band LC decline rates for our 197 SNe. Only 69 of the SNe Ia in our sample have available Δm_{15} values.

Table A5 provides our database of 197 individual SNe Ia (SN designation, U and V , spectroscopic subclass and Δm_{15} with their sources) and their 196 hosts (galaxy designation, distance, morphological type, R_{25} , and Z_{25}).

3 RESULTS AND DISCUSSION

3.1 Directional distributions of SNe Ia in edge-on spiral hosts

Following Hakobyan et al. (2021), for the SNe Ia in edge-on spirals of the current study, we perform the two-sample KS and AD tests comparing the $|V|/R_{25}$ and $|U|/R_{25}$ distributions between each other. Table 1 shows that the bulk of SNe Ia in all of the SN subclasses are localized in the host galaxies’ discs. For 91bg-like SNe only, the AD test shows barely significance, unlike the KS test, which is probably due to the statistics with the smallest sample size.

We then compare the projected and normalized radii $|U|/R_{25}$ and the heights $|V|/R_{25}$ between different SN Ia subclasses. In Table 2, the KS and AD tests show that the radial distributions of normal, 91T- and 91bg-like SNe are consistent with one another. In addition, the height distributions of normal and 91T-like SNe are consistent between each other. At the same time, the height distributions of 91T- and 91bg-like SNe are significantly different. The same is happens for the distributions of normal and 91bg-like SNe (with barely KS test significance). Fig. 1 shows a scatterplot of $|V|/R_{25}$ versus $|U|/R_{25}$, and the cumulative distributions of $|V|/R_{25}$ values for different SN Ia subclasses. The 91T-like SNe have the smallest height distributions, closest to the disc plane, whereas the 91bg-like SNe

¹ The sources provide also the equatorial coordinates of the selected SNe Ia.

² We used a 5 per cent significance level as the threshold for the tests.

Table 2. Comparison of the $|U|/R_{25}$ and $|V|/R_{25}$ distributions between different subclasses of SNe Ia.

Subsample 1	N_{SN}	versus	Subsample 2	N_{SN}	$P_{\text{KS}}^{\text{MC}}$	$P_{\text{AD}}^{\text{MC}}$
$ U /R_{25}$ of Normal	144	versus	$ U /R_{25}$ of 91bg	23	0.279	0.166
$ U /R_{25}$ of Normal	144	versus	$ U /R_{25}$ of 91T	30	0.828	0.835
$ U /R_{25}$ of 91bg	23	versus	$ U /R_{25}$ of 91T	30	0.756	0.611
$ V /R_{25}$ of Normal	144	versus	$ V /R_{25}$ of 91bg	23	0.079	0.010
$ V /R_{25}$ of Normal	144	versus	$ V /R_{25}$ of 91T	30	0.685	0.588
$ V /R_{25}$ of 91bg	23	versus	$ V /R_{25}$ of 91T	30	0.033	0.022

Notes. The explanations for the P -values are identical to those in Table 1.

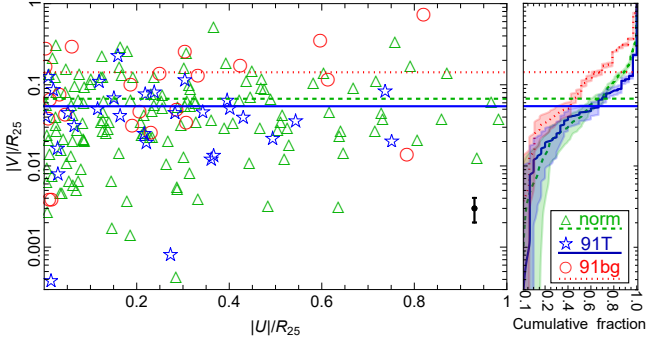


Figure 1. Left panel: distributions of $|V|/R_{25}$ versus $|U|/R_{25}$ for normal, 91T-, and 91bg-like SNe. The error bar on the right side of the panel shows the characteristic error in the height estimation due to possible inclination floating in $80^\circ - 90^\circ$. The lines show the mean $|V|/R_{25}$ values for each SN Ia subclass. Right panel: the heights' cumulative distributions for different SNe Ia. The light coloured regions around each curve represent the appropriate spreads considering the uncertainties in height measurements.

have the highest distribution (see also the $\langle |V|/R_{25} \rangle$ values in Table 1). Normal SNe Ia have a height distribution that is somewhat between those of the two others, but closer to 91T-like events.

The results, in Table 1, are in agreement with those of our previous papers (H17, Hakobyan et al. 2016, 2021). As already stated, the disc, rather than the spherical component, is where the majority of normal, 91T- and 91bg-like SNe Ia in spiral galaxies arise. In particular, Childress et al. (2014) showed that SN Ia progenitor age distribution in spirals peaks up to several hundred Myr (< 1 Gyr) and has a long tail up to ~ 10 Gyr, implying that the bulk of progenitors come from young/intermediate stellar component (e.g. Maoz & Mannucci 2012), which is mostly found in discs (e.g. Breda & Papaderos 2018). Although the old stars (> 1 Gyr) are distributed in both disc and spherical components of spiral galaxies, most of the old progenitors of SNe Ia also distributed in discs, as evidenced by the behaviour of the bulge to disc (B/D) flux ratio (e.g. Graham & Worley 2008) or mass ratio (e.g. Breda & Papaderos 2018). For example, the B/D flux ratio in the K -band, which is a tracer of the old population, decreases passing from early- to late-type spirals (e.g. Graham & Worley 2008): the average B/D flux ratios are ~ 0.33 and ~ 0.07 for S0/a–Sbc and Sc–Sdm galaxies, respectively.

Now let us look at the results in Table 2. Recall that we only use edge-on host galaxies, therefore it is practically impossible to correct the discs for the inclination effect and properly study the de-projected radial distributions of SNe. This could explain why the projected radial distributions of normal, 91bg, and 91T-like SNe are all consistent (see Table 2), although it is known that the ages

and other parameters of various stellar populations in spiral galaxies demonstrate radial dependency (e.g. González Delgado et al. 2015).

Table 2 also shows, statistically, that 91T- and 91bg-like SNe Ia are distributed differently toward the plane of their host disc. The mean heights are growing, starting with 91T-like events and progressing through normal and 91bg-like SNe (Table 1). On the other hand, it is well-known that spiral galaxies have a vertical stellar age gradient, with the age increasing as the vertical distance from the disc plane increases (e.g. Seth et al. 2005; Yoachim & Dalcanton 2006; Ciucă et al. 2018). Therefore, from the perspective of the vertical distribution (an age tracer) it may be deduced that the progenitors of 91T-like and normal SNe Ia are relatively younger than those of 91bg-like events. At least the age differences should be significant for 91T- versus 91bg-like SNe (Table 2, Fig. 1). The results are unaffected when the Z_{25} normalization is applied (Table A2). We emphasize that the current study is the first to demonstrate the observational differences in the heights of the SN Ia subclasses.

In fact, more luminous 91T-like SNe could be found more easily at the brighter host galaxy background than less luminous 91bg-like events. This would mean that 91T-like SNe could be observed closer to the disc than 91bg-like. If so, the observed effect would be a selection bias. However, it is crucial to note that 91T-like SNe are not as frequently detected at higher heights as 91bg-like (see Fig. 1). More luminous 91T-like SNe would undoubtedly be found if they had exploded at the higher heights from the disc. Hence, it is likely that the detection of 91T-like SNe at lower heights as opposed to 91bg-like is a real effect rather than the product of the mentioned selection bias. This is further supported by the observation that 91T-like SNe are mostly associated with star-forming environments (e.g. Raskin et al. 2009; Ruiter et al. 2013; H20) than 91bg-like SNe, which are more frequently seen in older environments (e.g. Panther et al. 2019). On the other hand, the star-forming environment has the lowest height in the galactic disc (e.g. Jurić et al. 2008).

3.2 Constraining the age of SN Ia progenitors

It is noteworthy that along with the qualitative age constraints of SN Ia progenitors we can add also quantitative ones. Table A3 compares the scale heights of SN Ia subclasses in our sample with the exponential scale heights of the MW thin and thick discs, as well as with those of 141 edge-on S0/a–Sd galaxies from Comerón et al. (2018), sampled according to the different morphological groups. The scale height of CC SNe in late-type host galaxies is also shown from our previous paper H17. Here an exponential vertical distribution $\exp(-|z|/\tilde{H})$ is used, where the scale height \tilde{H} is normalized to the galaxy R_{25} radius. The scale height of SNe $\tilde{H}_{\text{SN}} = \langle |V|/R_{25} \rangle$ for an exponential vertical distribution (see H17, for more details). Because the scale height of a stellar population depends on the morphological type of galaxies, being larger in early-types (e.g. Yoachim & Dalcanton 2006; Bizyaev et al. 2014), we split the sample into early- and late-type hosts in Table A3 to accurately compare different scales. Note that in spiral galaxies the majority of 91T-like events are found in Sb–Sdm (late-type) morphological bin, while most of normal SNe Ia and 91bg-like events are distributed in S0/a–Sc (early-type) bin (Table A1, see also H20).

As shown in Table A3, in early-type spirals, the scale height of normal SNe Ia is found between those of the thick and thin discs, while the scale height of 91bg-like events is clearly consistent with the thick disc. In late-type spirals, the scale height of 91T-like SNe Ia is close to that of CC SNe, while being larger. The average height of normal SNe Ia again is between thin and thick discs. The scale height of 91bg-like events again is in agreement with those of thick

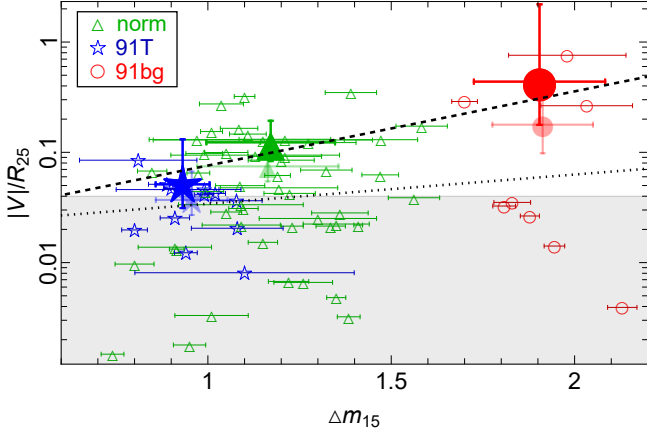


Figure 2. Distributions of $|V|/R_{25}$ versus Δm_{15} for different SN Ia subclasses. The dotted and dashed lines, which encompass all SN Ia subclasses, present the best-fitting lines for entire and dust-truncated (outside the shaded area) discs, respectively. Averaged values of $|V|/R_{25}$ (and Δm_{15}) with their 95 per cent CIs (and 1σ errors) for entire and dust-truncated samples are presented by medium-transparent and big-filled symbols, respectively.

discs. This is a rough comparison when taking into account the error bars of the mean heights, it nevertheless gives us a numerical understanding of the relative vertical distributions of SN subclasses in comparison with thin and thick components of galactic disc.

On the other hand, [Yoachim & Dalcanton \(2006\)](#) found that the scale height of thin disc of 34 late-type spiral galaxies corresponds to those of young/intermediate stellar populations with ages from ~ 10 Myr up to a few Gyr, while the scale height of thick disc is comparable to those of old stellar population with ages from a few Gyr up to ~ 10 Gyr (see also [Seth et al. 2005](#); [Yoachim & Dalcanton 2008](#)). A similar result was obtained by [Comerón \(2021\)](#) for the thick disc, where the age of stellar population increases from ~ 5 to ~ 10 Gyr (see also [Comerón et al. 2015, 2018](#); [Kasparova et al. 2016](#)). Similarly, the ages of stellar populations of the MW thin and thick discs are estimated to be up to a few Gyr and from a few Gyr up to ~ 10 Gyr, respectively (e.g. [Bensby et al. 2007](#); [Jurić et al. 2008](#)). Notably, CC SNe arise from young progenitors with ages up to ~ 100 Myr and their vertical extend is accordingly less than the thin disc ([H17](#)).

Thus, the various SN Ia subclasses correspond to different stellar population ages being distributed at the various average heights from the disc (e.g. [Seth et al. 2005](#); [Yoachim & Dalcanton 2008](#); [H17](#)). From [Table A3](#), we can impose rough numerical constraints on the SN progenitors: 91T-like events arise from progenitors with ages about several 100 Myr, the ages of progenitors of 91bg-like SNe are comparable to ~ 10 Gyr, while normal SNe Ia arise from progenitors with ages from about one up to ~ 10 Gyr.

It is important to note that the delay time³ of the SN progenitor system could be dominated by the timescale of the gravitational inspiral of WDs in comparison with the stellar age (a lifetime till it becomes WD, see [Hillebrandt et al. 2013](#); [Livio & Mazzali 2018](#)). In this study, however, we consider the stellar age of SN progenitors rather than the system’s entire delay time when comparing their average heights with those of various disc components. Note that a significant change in the mean vertical scales of the young and old

³ Time interval between the progenitor formation and the SN explosion.

Table 3. The correlation test for the $|V|/R_{25}$ versus Δm_{15} parameters.

SN	N_{SN}	$\langle V /R_{25} \rangle$	versus	$\langle \Delta m_{15} \rangle$	r_s	P_s^{MC}
All	69	$0.08^{+0.02}_{-0.02}$	versus	1.21 ± 0.32	0.118	0.334
All†	36	$0.14^{+0.06}_{-0.04}$	versus	1.18 ± 0.29	0.471	0.004

Notes. A coefficient of Spearman’s rank correlation ($r_s \in [-1; 1]$) is a metric for determining how closely two variables are related by a monotonic function. The variables are not independent when $P \leq 0.05$ (highlighted in bold). The P_s^{MC} values are generated using permutations with 10^5 MC iterations. The subsample marked with † symbol corresponds to SNe with $|V|/R_{25} \geq 0.04$.

stellar populations is not expected during the SN progenitor stellar age or the delay time of the systems. As mentioned above, 91T-like events (and the most of normal SNe Ia) are associated with star-forming environments ($\lesssim 500$ Myr; [Raskin et al. 2009](#); [Ruiter et al. 2013](#)), therefore the effect of the gravitational inspiral’s timescale should play a role mostly for 91bg-like SNe.

3.3 Relating LC decline rates with SN heights from host disc

SNe Ia span a variety of properties from subluminescent SNe with fast-declining LCs to overluminous and slowly evolving events (e.g. [Taubenberger 2017](#)). The majority of earlier theoretical studies have failed to fit the full range of observed SNe Ia properties with a single explosion/progenitor scenario (see reviews by [Hillebrandt et al. 2013](#); [Livio & Mazzali 2018](#)). Fortunately, recent theoretical studies in the sub- M_{Ch} WD explosion models showed an excellent quantitative agreement with observed photometrical behaviours of SNe Ia in the entire range of the [Phillips relation](#) (e.g. [Blondin et al. 2017](#); [Shen et al. 2017, 2021](#)). As mentioned in the Introduction, the explosion is realized in the double detonation of a sub- M_{Ch} WD, where the LC decline rate Δm_{15} of SN Ia is positively correlated with the age of the SN progenitor system (e.g. [Shen et al. 2017, 2021](#)).

Numerous researches extensively studied the links between the SNe Ia LC decline rates and the global age (or age tracers) of host galaxies, as well as local age at SN explosion sites (e.g. [Howell et al. 2009](#); [Gupta et al. 2011](#); [Pan et al. 2014](#); [Ashall et al. 2016](#); [Roman et al. 2018](#); [H20](#)). These studies demonstrated that, at different levels of significance, the LC decline rate is correlated with the global/local age: the B -band Δm_{15} values increase with stellar population age. However, the correlation between SNe Ia decline rate and the height from the host disc, which is a reliable age indicator of stellar population, has not yet been investigated. Here, we intend to fill this gap.

[Fig. 2](#) and the Spearman’s rank correlation test in [Table 3](#) show that the trend between $|V|/R_{25}$ and Δm_{15} is positive, but not statistically significant. At low heights, in [Fig. 2](#), we observe all the SN Ia subclasses (full range with slower and faster declining LCs), but with increasing height, the decline rate of objects increases on average. However, it should be taken into account that due to the dust extinction in galactic disc the discovery of SNe Ia in edge-on galaxies is complicated and biased against objects at lower heights from the disc (e.g. [Holwerda et al. 2015](#)). The impact of this effect would be greatest on subluminescent SNe (91bg-like events).

In late-type galaxies, the vertical distribution of dust has a scale height that is ~ 3 times less than that of thick disc stars (e.g. [Bianchi 2007](#)). While the dust layer is ~ 1.5 times thicker in early-type galaxies (e.g. [Hacke et al. 1982](#); [De Geyter et al. 2014](#)), which is closer to our sample of SNe Ia host galaxies (see [Table A1](#)). Therefore, to avoid the possible impact of dust we truncate the heights of SNe with $|V|/R_{25} \geq 0.04$, leaving 36 SNe Ia in our sample. For

this dust-truncated sample, the Spearman's rank test reveals a significant positive correlation between the $|V|/R_{25}$ and Δm_{15} parameters (Table 3, Fig. 2). The results are unaffected when the Z_{25} normalization is applied (Table A4). Thus, despite the limited sample size, we demonstrate for the first time a significant correlation between LC decline rates and SNe Ia heights, which is consistent with a sub- M_{Ch} WD explosion models (e.g. Sim et al. 2010; Blondin et al. 2017; Shen et al. 2017) and vertical age gradient of stellar population in discs (e.g. Yoachim & Dalcanton 2006; Ciucă et al. 2018).

It would be important to verify the results in Tables 2 and A2 while accounting for the selection effects brought by dust extinction. However, in these tables we compare the SN positions (importantly heights) between the subclasses, and after the dust-truncation the samples for 91T- and 91bg-like SNe become, unfortunately, insufficient to perform the statistical tests.

4 CONCLUSIONS

In this Letter, we analyse the height distributions of SN Ia subclasses (normal, 91T- and 91bg-like) from their host disc plane using spectroscopically classified 197 SNe in edge-on spiral galaxies with distances ≤ 200 Mpc. In addition, this study is performed to examine potential links between photometric characteristics of SNe Ia, like LC decline rates (Δm_{15}), and SN heights from the disc.

For the first time, we demonstrate that 91T- and 91bg-like subclasses of SNe Ia are distributed differently toward the plane of their host edge-on disc. On average, the SN heights are rising, beginning with 91T-like events and progressing through normal and 91bg-like SNe Ia. Considering that the height from the disc is a stellar population age indicator and comparing the mean heights of the SN Ia subclasses with those of thin and thick discs with known ages, we roughly estimate that 91T-like events originate from relatively younger progenitors with ages of about several 100 Myr, the ages of progenitors of normal SNe Ia are from about one up to ~ 10 Gyr, and 91bg-like SNe Ia arise from progenitors with significantly older ages ~ 10 Gyr. In addition, we show that the SN Ia LC decline rates correlate with their heights from the host disc, after excluding the selection effects brought by dust extinction. The observed correlation is consistent with the explosion models of a sub- M_{Ch} mass WD (e.g. Blondin et al. 2017; Shen et al. 2017, 2021) and the vertical age gradient of stellar population in discs (e.g. Seth et al. 2005; Yoachim & Dalcanton 2006; Ciucă et al. 2018).

Fortunately, a far larger spectroscopic and photometric sample of nearby SNe Ia will be made available by the ongoing robotic telescope surveys at various locations throughout the globe (e.g. All Sky Automated Survey for SuperNovae) and by the forthcoming Vera C. Rubin Observatory (the Large Synoptic Survey Telescope), which will allow for statistically more powerful and accurate analysis.

ACKNOWLEDGEMENTS

We appreciate the anonymous referee's suggestions for enhancing our Letter. I thank my PhD supervisor Dr. Artur Hakobyan for his support. The work was supported by the Science Committee of RA, in the frames of the research project № 21T-1C236.

DATA AVAILABILITY

The data underlying this study may be found in the article's supplementary material online (see Table A5, for guidance).

REFERENCES

- Ahumada R., et al., 2020, *ApJS*, 249, 3
 Ashall C., Mazzali P., Sasdelli M., Prentice S. J., 2016, *MNRAS*, 460, 3529
 Bensby T., Zenn A. R., Oey M. S., Feltzing S., 2007, *ApJ*, 663, L13
 Bianchi S., 2007, *A&A*, 471, 765
 Bizyaev D. V., Kautsch S. J., Mosenkov A. V., Reshetnikov V. P., Sotnikova N. Y., Yablokova N. V., Hillyer R. W., 2014, *ApJ*, 787, 24
 Blondin S., Dessart L., Hillier D. J., Khokhlov A. M., 2017, *MNRAS*, 470, 157
 Breda I., Papaderos P., 2018, *A&A*, 614, A48
 Chambers K. C., et al., 2016, preprint, ([arXiv:1612.05560](https://arxiv.org/abs/1612.05560))
 Childress M. J., Wolf C., Zahid H. J., 2014, *MNRAS*, 445, 1898
 Ciucă I., Kawata D., Lin J., Casagrande L., Seabroke G., Cropper M., 2018, *MNRAS*, 475, 1203
 Comerón S., 2021, *A&A*, 645, L13
 Comerón S., Salo H., Janz J., Laurikainen E., Yoachim P., 2015, *A&A*, 584, A34
 Comerón S., Salo H., Knapen J. H., 2018, *A&A*, 610, A5
 De Geyter G., Baes M., Camps P., Fritz J., De Looze I., Hughes T. M., Viaene S., Gentile G., 2014, *MNRAS*, 441, 869
 González Delgado R. M., et al., 2015, *A&A*, 581, A103
 Graham A. W., Worley C. C., 2008, *MNRAS*, 388, 1708
 Guillochon J., Parrent J., Kelley L. Z., Margutti R., 2017, *ApJ*, 835, 64
 Gupta R. R., et al., 2011, *ApJ*, 740, 92
 Hacke G., Schielicke R., Schmidt K. H., 1982, *Astron. Nachr.*, 303, 245
 Hakobyan A. A., et al., 2016, *MNRAS*, 456, 2848
 Hakobyan A. A., et al., 2017, *MNRAS*, 471, 1390 (H17)
 Hakobyan A. A., Barkhudaryan L. V., Karapetyan A. G., Gevorgyan M. H., Mamon G. A., Kunth D., Adibekyan V., Turatto M., 2020, *MNRAS*, 499, 1424 (H20)
 Hakobyan A. A., Karapetyan A. G., Barkhudaryan L. V., Gevorgyan M. H., Adibekyan V., 2021, *MNRAS*, 505, L52
 Hillebrandt W., Kromer M., Röpke F. K., Ruiter A. J., 2013, *Front. Phys.*, 8, 116
 Holwerda B. W., Reynolds A., Smith M., Kraan-Korteweg R. C., 2015, *MNRAS*, 446, 3768
 Howell D. A., 2001, *ApJ*, 554, L193
 Howell D. A., et al., 2009, *ApJ*, 691, 661
 Jurić M., et al., 2008, *ApJ*, 673, 864
 Kasparova A. V., Katkov I. Y., Chilingarian I. V., Silchenko O. K., Moiseev A. V., Borisov S. B., 2016, *MNRAS*, 460, L89
 Li W., et al., 2011, *MNRAS*, 412, 1441
 Livio M., Mazzali P., 2018, *Phys. Rep.*, 736, 1
 Maoz D., Mannucci F., 2012, *PASA*, 29, 447
 Onken C. A., et al., 2019, *PASA*, 36, e033
 Pan Y. C., et al., 2014, *MNRAS*, 438, 1391
 Panther F. H., Seitzzahl I. R., Ruiter A. J., Crocker R. M., Lidman C., Wang E. X., Tucker B. E., Groves B., 2019, *PASA*, 36, e031
 Paturel G., et al., 1997, *A&AS*, 124
 Phillips M. M., 1993, *ApJ*, 413, L105
 Piro A. L., Thompson T. A., Kochanek C. S., 2014, *MNRAS*, 438, 3456
 Raskin C., Scannapieco E., Rhoads J., Della Valle M., 2009, *ApJ*, 707, 74
 Roman M., et al., 2018, *A&A*, 615, A68
 Ruiter A. J., et al., 2013, *MNRAS*, 429, 1425
 Seth A. C., Dalcanton J. J., de Jong R. S., 2005, *AJ*, 130, 1574
 Shen K. J., Toonen S., Graur O., 2017, *ApJ*, 851, L50
 Shen K. J., Kasen D., Miles B. J., Townsley D. M., 2018, *ApJ*, 854, 52
 Shen K. J., Blondin S., Kasen D., Dessart L., Townsley D. M., Boos S., Hillier D. J., 2021, *ApJ*, 909, L18
 Sim S. A., Röpke F. K., Hillebrandt W., Kromer M., Pakmor R., Fink M., Ruiter A. J., Seitzzahl I. R., 2010, *ApJ*, 714, L52
 Stritzinger M., Leibundgut B., Walch S., Contardo G., 2006, *A&A*, 450, 241
 Taubenberger S., 2017, in Alsabti A. W., Murdin P., eds, *The Extremes of Thermonuclear Supernovae*, Handbook of Supernovae. Springer, p. 317
 Yaron O., Gal-Yam A., 2012, *PASP*, 124, 668
 Yoachim P., Dalcanton J. J., 2006, *AJ*, 131, 226
 Yoachim P., Dalcanton J. J., 2008, *ApJ*, 683, 707

Table A1. Broadly binned morphological distribution of SN Ia subclasses in edge-on spiral host galaxies.

SN	S0/a–Sab	Sb–Sc	Scd–Sdm	All
Normal	46	81	17	144
91T	5	18	7	30
91bg	13	10	0	23
All	67	108	22	197

Table A2. Comparison of the $|V|/Z_{25}$ distributions between different subclasses of SNe Ia.

Subsample 1	N_{SN}	versus	Subsample 2	N_{SN}	$P_{\text{KS}}^{\text{MC}}$	$P_{\text{AD}}^{\text{MC}}$
Normal	144	versus	91bg	23	0.112	0.005
Normal	144	versus	91T	30	0.311	0.307
91bg	23	versus	91T	30	0.042	0.048

Notes. The explanations for the P -values are identical to those in Table 1.

Table A3. Comparison of exponential scale heights of SN Ia subclasses with those of CC SNe, and thick and thin discs of edge-on galaxies.

Disc	N	\tilde{H}	Reference
Early-type galaxies			
S0/a–Sc thin disc	122	$0.02^{+0.01}_{-0.01}$	Comerón et al. (2018)
S0/a–Sab thin disc	38	$0.04^{+0.02}_{-0.01}$	Comerón et al. (2018)
Normal (S0/a–Sab)	46	$0.07^{+0.03}_{-0.02}$	This study
S0/a–Sc thick disc	122	$0.11^{+0.02}_{-0.02}$	Comerón et al. (2018)
91bg (S0/a–Sc)	23	$0.14^{+0.08}_{-0.04}$	This study
91bg (S0/a–Sab)	13	$0.16^{+0.15}_{-0.06}$	This study
S0/a–Sab thick disc	38	$0.17^{+0.07}_{-0.04}$	Comerón et al. (2018)
Late-type galaxies			
MW thin disc		0.02 ± 0.01	Jurić et al. (2008)
Sb–Sc thin disc	84	$0.02^{+0.01}_{-0.01}$	Comerón et al. (2018)
CC SNe	27	$0.03^{+0.02}_{-0.01}$	H17
91T (Sb–Sdm)	25	$0.04^{+0.02}_{-0.01}$	This study
Normal (Scd–Sdm)	17	$0.05^{+0.04}_{-0.02}$	This study
MW thick disc		0.06 ± 0.01	Jurić et al. (2008)
Normal (Sb–Sc)	81	$0.07^{+0.02}_{-0.01}$	This study
Scd–Sd thick disc	19	$0.08^{+0.06}_{-0.03}$	Comerón et al. (2018)
Sb–Sc thick disc	84	$0.08^{+0.02}_{-0.02}$	Comerón et al. (2018)
91bg (Sb–Sc)	10	$0.12^{+0.13}_{-0.05}$	This study

Notes. $\tilde{H}_{\text{SN}} = \langle |V|/R_{25} \rangle$. Morphological classification of galaxies from Comerón et al. (2018) is available via the HyperLeda and/or NED. The \tilde{H} values are displayed in ascending order.

APPENDIX A: ONLINE MATERIAL

Table A1 shows broadly binned morphological distribution of SN Ia subclasses in edge-on spiral galaxies. Table A2 compares the $|V|/Z_{25}$ distributions between different subclasses of SNe Ia. Table A3 compares the exponential scale heights of SN Ia subclasses with those of CC SNe, and thick and thin discs of galaxies. Table A4 shows the correlation test for the $|V|/Z_{25}$ versus Δm_{15} parameters.

A portion of the database underlying the study is shown in Table A5 for guidance regarding its content and format. The entire table is available in electronic format as an CSV file.

Table A4. The correlation test for the $|V|/Z_{25}$ versus Δm_{15} parameters.

SN	N_{SN}	$\langle V /Z_{25} \rangle$	versus	$\langle \Delta m_{15} \rangle$	r_s	P_s^{MC}
All	69	$0.24^{+0.07}_{-0.05}$	versus	1.21 ± 0.32	0.058	0.633
All†	36	$0.41^{+0.18}_{-0.11}$	versus	1.18 ± 0.29	0.396	0.016

Notes. For the explanations of the parameters see Table 3. The subsample marked with † symbol corresponds to the dust-truncated SNe with $|V|/Z_{25} \geq 0.123$. For our host galaxy sample, the truncation is obtained by considering that $\langle Z_{25}/R_{25} \rangle \approx 0.325$.

Table A5: The database of 197 SNe Ia and their 196 host galaxies. The first ten entries are displayed. The full table can be found in the article's online version.

SN	Subclass	Source Bibcode	U arcsec	V arcsec	Δm_{15} mag	Source Bibcode	Host	Dist. Mpc	Morph.	R_{25} arcsec	Z_{25} arcsec
1959C	norm	1993AJ....106.2383B	8.340	0.066	0.74 ± 0.07	2017ApJ...835...64G	MCG+01-34-005	42.563	Sc	44.826	11.715
1962J	norm	1993AJ....106.2383B	40.100	13.776	1.01 ± 0.07	2017ApJ...835...64G	NGC6835	20.201	Sab	89.277	29.850
1984A	norm	2009ApJ...699L.139W	25.132	13.913	1.21 ± 0.10	2005ApJ...623.1011B	NGC4419	16.095	Sa	105.893	44.721
1990G	norm	2012MNRAS.425.1789S	35.170	5.912	-	-	IC2735	153.410	Sab	40.386	14.789
1991bd	norm	2012MNRAS.425.1789S	35.801	6.736	-	-	UGC02936	51.771	Sc	117.645	22.623
1991bf	norm	2012MNRAS.425.1789S	25.416	1.118	-	-	ESO471-030	120.768	Sa	39.665	17.126
1991K	91T	2012MNRAS.425.1789S	18.898	7.251	-	-	NGC2851	70.776	S0/a	62.163	30.627
1992ag	norm	1992IAUC.5555....1M	2.849	2.067	1.19 ± 0.10	1996AJ....112.2408H	ESO508-067	104.045	Sb?	33.522	10.278
1993ah	norm	1993IAUC.5897....1B	7.661	0.914	1.30 ± 0.10	1996AJ....112.2408H	ESO471-027	120.357	Sab	36.384	13.386
1993L	norm	1993IAUC.5782....1D	23.490	4.488	1.47 ± 0.07	2005ApJ...624...532R	IC5270	23.387	Sbc	71.856	20.562

Notes. We more precisely identify the morphologies of edge-on galaxies by assessing the size of the bulge relative to the disc (see H17).